Non-Isothermal Dehydration Kinetics of Diphasic Mullite Precursor Gel

Roy, Jagannath*+

Central University of South Bihar, Gaya, INDIA

Maitra, Saikat

Maulana Abul Kalam Azad University of Technology, Kalyani, INDIA

ABSTRACT: *Aluminosilicate gel precursor having mullite composition was synthesized from inorganic salts of aluminum and silicon by employing the sol-gel method. Chemical analysis, surface area and bulk density measurements were performed to characterize the dried gel. The course of the mullitization was examined by FT-IR analysis which confirmed the diphasic nature of the gel. SEM and XRD analysis were preformed to study microstructure and phase development. ThermoGravimetric (TG) analysis of the dried gel was performed at multiple heating rates and from the results obtained; kinetics of thermal dehydration was studied by applying Friedman differential and Kissinger-Akahira-Sunose integral isoconversional procedures. It was observed that the total dehydration process of the gel was accomplished by two different stages and both the stages followed second order rate kinetics. The first stage was assigned to the dehydration of silicon hydroxide gel whereas the second stage was associated with aluminum hydroxide gel dehydration.*

KEYWORDS: *Sol-gel process; Dehydration kinetics; Activation energy; Friedman method; Kissinger-Akahira-Sunose approximation.*

INTRODUCTION

ThermoGravimetric (TG) analysis has been widely used for the study of solid state reactions. In the non-isothermal analysis, the mass loss of a sample under heat treatment is measured against the temperature under a controlled heating rate. From the thermograms, the kinetic parameters can be calculated as the shape of these curves is the function of reaction kinetics. To get information about kinetic parameters, several model fitting (a reaction model has to be chosen) and model free (does not require a reaction model) kinetic calculations method were developed.

The sol-gel process is one of the most advanced methods to synthesize powders with better homogeneity and more purity compared with other conventional methods. During dehydration of the gel, with increasing temperature, water and other volatiles compounds are vaporized leaving behind the solid residues. This dehydration process can be well studied by thermogravimetric analysis. A number of works have been reported on the dehydration kinetics of synthetic gels based on the thermogravimetric analysis. Some of these reported works are mentioned here.

* *To whom correspondence should be addressed.*
+ *E-mail: royj0707@gmail.com*
1021-9986/2019/4/91-100 10/$/6.00

Catauro et al. employed the sol-gel method to synthesize $SiO_2.CaO.P_2O_5$ materials and studied the thermal behavior by ThermoGravimetry and Differential Thermal Analysis (TG/DTA). Integral isoconversional kinetic method of Ozawa-Flynn-Wall with Doyle approximation was used to study the dehydration kinetics of the gel [1]. Hernandez-Escolano et al. [2] performed TG analysis of a gel sample and used model free integral isoconversional non-isothermal procedure for kinetic study. The n=6 kinetic model was observed to be the best fit for all the system. Biedunkiewicz et al. [3] performed TG-DSC measurements under non-isothermal and isothermal conditions at four different temperatures and used the Coats-Redfern method to describe the kinetic parameters. *Maitra et al.* [4] synthesized zeolite gel and showed that gel dehydration followed first order kinetics and it proceeded through low energy diffusion controlled process. *Budrugeac et al.* [5] studied non-isothermal kinetics of decomposition of zinc-acetate based gel precursors using thermogravimetric data. The invariant Kinetic Parameter (IKP) method was used for evaluating activation energy, pre exponential factor and kinetic model. It was observed that decomposition of the gel sample followed F1 kinetic model. *Want et al.* [6] performed the thermogravimetric and differential thermal analysis of gel grown single crystal of ytterbium tartrate hydrate. The decomposition of the gel was started after 200ºC and completed in two stages at around 700ºC. By using the integral method and applying the Coats-Redfern approximation, the non-isothermal kinetics parameters like activation energy and frequency factors were evaluated. *Jankovic et al.* [7] studied the dehydration process of swollen polyhydrogel at different heating rates. Under the non-isothermal conditions, different kinetic parameters like activation energy, pre-exponential factor and kinetic model for the hydrogel dehydration process were studied by applying methods like Kissinger, Coats-Redfern, etc.

In spite of these different reported works, little information is available on the dehydration kinetics of synthetic aluminosilicate gel. Highly pure aluminosilicate compound with mullite composition can show excellent resistance to heat, high strength, chemical, and thermal stability, low thermal expansion coefficient, [8-12] etc. Mullite is an important material as it has uses in manufacturing refractory materials, optical and electrical components, porous coatings, biological processes, separation and purification of membranes, [13-16] etc. So in this present investigation, thermogravimetric analysis of aluminosilicate gel was performed at four different heating rates and the kinetic triplet (reaction order, activation energy and frequency factor) was calculated using the Friedman method. The results were further verified by Kissinger-Akahira-Sunose (KAS) approximation method.

EXPERIMENTAL SECTION

Synthesis of the gel

To synthesize aluminosilicate hydrogel (Al_2O_3: SiO_2 = 3:2), analar grade of 5% (w/v) aluminum nitrate nonahydrate [Al $(NO_3)_3$. $9H_2O$, (MERCK, India), alumina content 12.98% w/w] and 5% (w/v) liquid sodium silicate [sp. Gr. 1.6 and molar ratio of Na_2O: SiO_2 =1:3, (LOBA CHEMIE, India), silica content 29.75% w/w] were used as the starting materials. From liquid sodium silicate, silicic acid was prepared by passing a solution of sodium silicate (7% w/v) through a column packed with Dowex-50 cation exchanging resin with a flow rate of 200 mL/minute. Silica sol was prepared by ultrasonic dispersion of the generated silicic acid in the aqueous phase. Silica sol was mixed with $Al(NO_3)_3.9H_2O$ solution by maintaining alumina and silica ratio of mullite composition. At this moment, the pH of the solution was 2. Now ammonia solution (1:1) was added slowly in the mixed solution with constant stirring until pH of the solution was reached at around 9. The mixed sol was then filtered, washed thoroughly and allowed to age to form a gel. Now the gel was dried at 80°C for overnight.

Characterization of the gel

Chemical analysis was performed by following the specification laid in ISO 21587-2:2007 [17]. The surface area was determined using Twin Surface area analyser, Quantachrome and bulk density was measured by using Ultrapyc 1200e Helium Pyconnometer. Fourier Transformation InfraRed (FT-IR) spectroscopic analysis of the dried gel and heat treated samples (heat treated at eight different temperatures from 200 to 1600°C with an interval of 200°C each, was performed by using a Perkin-Elmer apparatus (Model: Vertex-70). ThermoGravimetric (TG) analysis of the dried gel was performed in a TGA-DSC

Thermal Analyzer (TA) module (Make and Model METTLER TOLEDO) at 4 different heating rates 4, 6, 8 and 10°C/min from room temperature to 800°C. The data were analyzed by STARe software. Differential thermal analysis (DTA) of the dried gel was performed with a differential thermal analyzer (Libratherm 1400, India) at four different heating rates 4, 6, 8 and 10°C/min from room temperature to 1200°C. Calcination of the dried gel was performed at 800°C for 2 hours followed by compaction under 100 MPa pressure. The compacted masses were then sintered at three different final temperatures (1400, 1500 and 1600 °C) and soaked for 2 hours at final temperatures. The heating rate was 10°C/min up to 1000°C followed by 2 °C/min up to final temperatures. XRD pattern of the sample was taken from the Rigaku X-ray diffractometer with Cu target (Miniflex, Japan) and SEM analysis was performed with FEI Quanta microscope (US).

Kinetic Calculations

Isoconversional kinetic calculations:

Dehydration of the gel can be represented by the following reaction scheme:

Gel → Solid residues + Volatiles

The fraction of dehydrated mass ‘α’ can be defined by the following expression:

$$\alpha=\frac{m_0-m_t}{m_0-m_f} \qquad (1)$$

Where m_0 is the mass of the gel at the beginning, m_t and m_f are refer to the masses at time‘t’ and at the end of the experiment respectively.

Now rate of dehydration (dα/dt), is a linear function of temperature-dependent rate constant (k), and reaction model (a temperature –independent function of conversion), f(α):

$$\frac{d\alpha}{dt}=kf(\alpha) \qquad (2)$$

Isoconversional calculation methods can be split into two different categories: differential and integral [15].

(i) Differential isoconversional methods-

Replacing the rate constant with Arrhenius equation ($k=A.e^{-\frac{E}{RT}}$), Equation (2) becomes:

$$\frac{d\alpha}{dt}=A.e^{-\frac{E}{RT}}f(\alpha) \qquad (3)$$

Where *A* is the pre-exponential factor, *E* is the activation energy, *R* is the universal gas constant and *T* is the absolute temperature.

By taking the logarithm of Equation (3), we can get,

$$\ln(\frac{d\alpha}{dt})=\ln[A.f(\alpha)]-\frac{E}{RT} \qquad (4)$$

This equation was proposed by *Friedman* [18]. Now by introducing heating rate ($\beta=\frac{dT}{dt}$) in the above equation and rearranging we can write,

$$\ln(\frac{d\alpha}{dT})-\ln[f(\alpha)]=\ln(\frac{A}{\beta})-\frac{E}{RT} \qquad (5)$$

The plot of $\ln(\frac{d\alpha}{dT})-\ln[f(\alpha)]$ versus $\frac{1}{T}$ should be a straight line. Now values of f(α) are chosen arbitrarily as available in the literature [19] and calculations were performed at all four heating rates. Now $\ln(d\alpha/dT)-\ln[f(\alpha)]$ values were plotted against $\frac{1}{T}$ and from these plots best fit value of f(α) was chosen which has the best correlation coefficient. Now from the plot of best fitted ‘f(α)’ value, activation energy and pre-exponential factor were calculated by taking slope =-$\frac{E}{R}$ and intercept= $\ln(A/\beta)$ at all four heating rates.

(ii) Integral isoconversional methods

Integration of equation (3) will give the following form [18],

$$g(\alpha)\equiv\int_0^\alpha\frac{d\alpha}{f(\alpha)}=\frac{A}{\beta}\int_0^T e^{(-\frac{E}{RT})}dT \qquad (6)$$

To get a solution of equation (6), several approximations were proposed. Kissinger-Akahira-Sunose (KAS) developed one such approximation and their proposed equation is the following [10],

$$\ln(\frac{\beta}{T^2})=\ln[\frac{AR}{g(\alpha).E}]-\frac{E}{RT} \qquad (7)$$

Where g(α) is the reaction model which depends on the conversion mechanism and its algebraic expression.

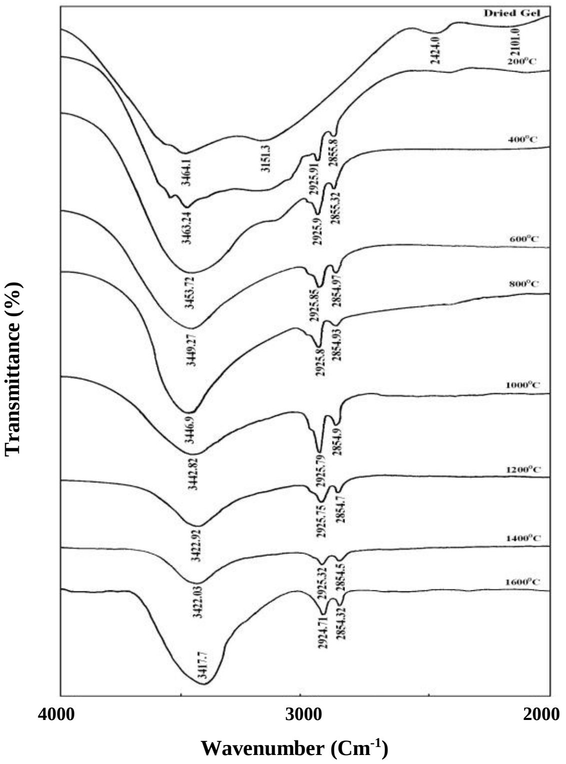

Fig. 1A: FTIR spectra of Al_2O_3-SiO_2 gel after heat treating at different temperatures within 2000-4000 cm^{-1} [20]

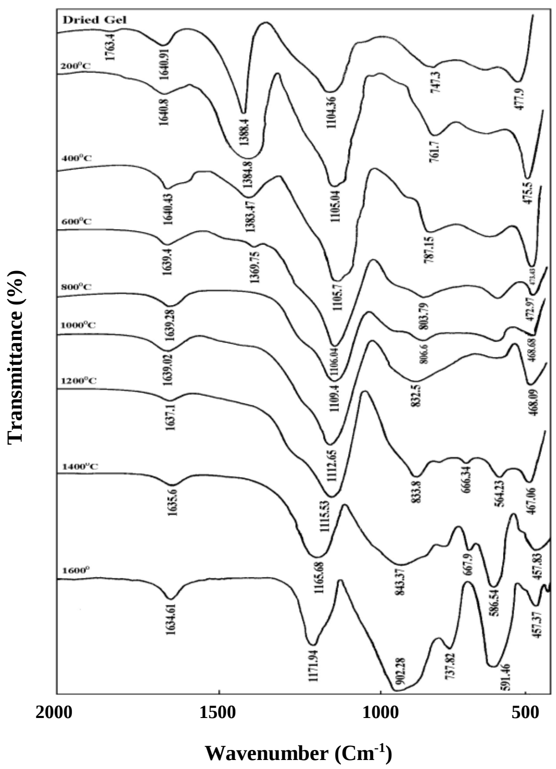

Fig. 1B: FTIR spectra of Al_2O_3-SiO_2 gel after heat treating at different temperatures within 400-2000cm^{-1} [20]

To determine the reaction order, Equation (7) is rearranged in the following way,

$$\ln\left[\frac{g(\alpha)}{T^2}\right]=\ln\left[\frac{AR}{\beta E}\right]-\frac{E}{RT} \quad (8)$$

Now the plot of $\ln\left[g(\alpha)/T^2\right]$ versus 1/T will be a straight line with slope equal to -1.0000. Using linear regressive of least square method and choosing arbitrary values of g(α) available in the literature [19], ln [$g(\alpha)/T^2$] values were plotted against 1/T and plot to have slope closet to -1.0000 and correlation coefficient closet to unity was considered as the best fit mechanism function of [g(α)]. Activation energy and frequency factor were determined by the method recommended by ICTAC kinetic committee [18]. Subsets of the TG-curves at certain values of α and corresponding temperatures were taken and the dependence of ln [β/T^2] on 1/T was drawn according to equation-7 for both stages. The activation energy E and frequency factor were determined from the slope and intercept of each plot using Equation (7).

RESULT AND DISCUSSION

The bulk density and surface area of the dried gel were found to be 0.27 g/cm^3 and 70m^2/g respectively. So formed gel is highly surface active. The gel contained almost 30% water and hence the gel was calcined before sintering to avoid excessive shrinkage. To prevent the formation of the glassy phase during sintering, the alumina content of the synthesized gel was intentionally kept slightly higher than the theoretical ratio of alumina and silica (3:2) in mullite.

FT-IR spectra of Al_2O_3-SiO_2 gel after heat treating at different temperatures have been presented in Fig-1A and 1B.

No characteristic peak of Al-O-Si linkage was observed in the FITR spectra. But peaks concerned with Al-O-Al and Si-O-Si stretching vibrations appeared at 747 cm^{-1} and 1104 cm^{-1}. These results confirm the diphasic nature of the gel during its formation. This means both aluminum hydroxide [$Al(OH)_3$] and silicon hydroxide [$Si(OH)_4$] gel were formed and precipitated simultaneously. The peak corresponding to the formation

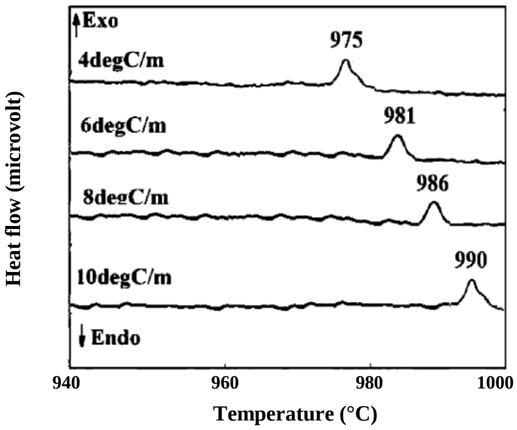

Fig. 2: DTA curves of Al_2O_3-SiO_2 gel at different heating rates [21].

of Al-O-Si linkage was first observed in the spectra of the gel hated at 600°C. Mullitization was found to start at around 1000°C and crystallization of mullite was completed after heating the sample at around 1600°C [20].

Differential Thermal Analysis (DTA) of the gel performed at the different heating rate indicated the exothermic nature of the mullitization process and the process was found to start in the temperature range between 975 to 990°C (Fig. 2).

In the x-ray diffractograms of the gel fired at 1400, 1500 and 1600°C, mullite was found to be the major phase followed by corundum and cristobalite (Fig. 3). However, the relative proportion of mullite phases was found to increase with an increase in sintering temperature.

The information obtained about the synthesized gel during FT-IR, DTA and XRD analysis have been discussed in our earlier work [20]. This study confirmed that the process of mullitization become more effective with increasing sintering temperature and after sintering at 1600°C, mullitization was found to complete.

From the Scanning Electron Micrographs (SEM) of the sintered samples (Fig. 4), it is apparent that undoped sol-gel mullite formed very small crystallites. It is further apparent that the microstructure contained a substantial portion of amorphous phases and the relative proportions of the amorphous phases in the sintered masses decreased as the sintering temperature was increased from 1400 to 1600 °C. The crystallite size became more prominent as the sintering temperature was increased.

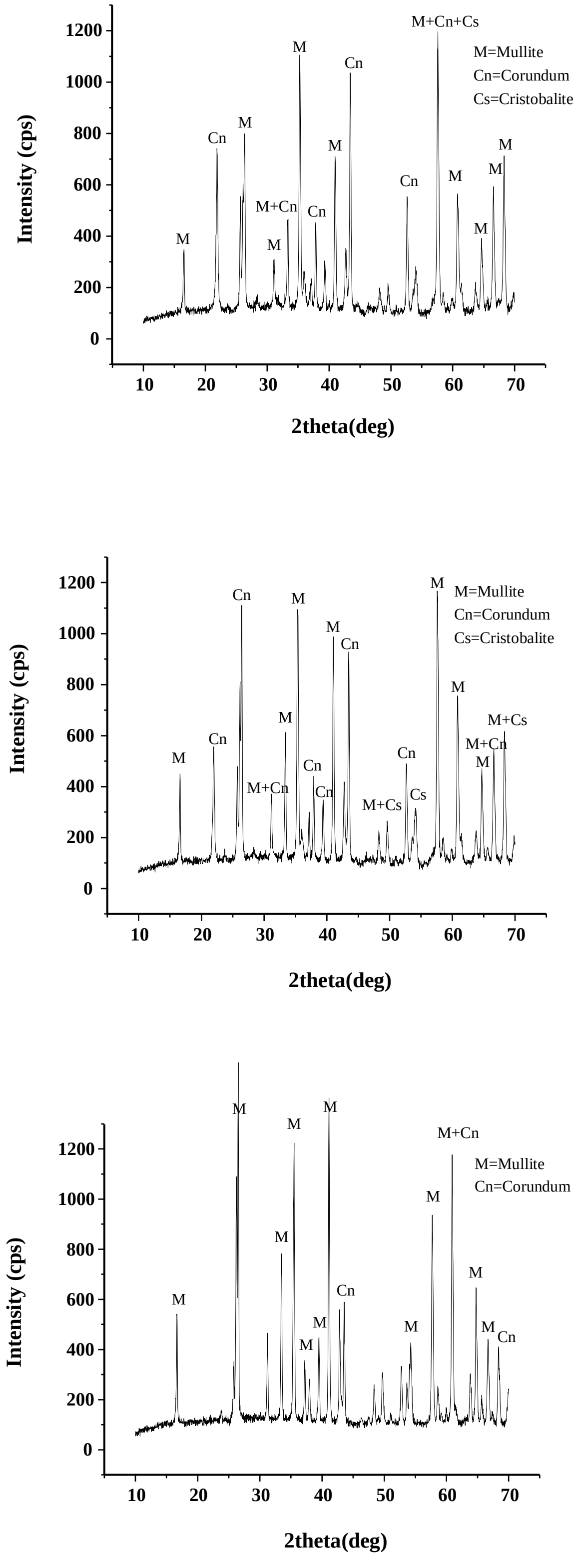

Fig. 3: XRD diagram of the aluminosilicate gel sintered at (i) 1400 C (ii) 1500°C (iii) 1600°C [21].

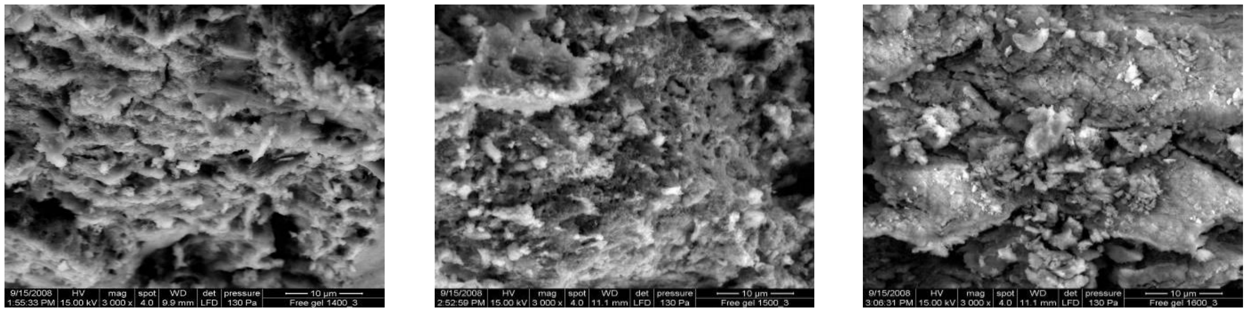

(a) (b) (c)

Fig. 4: SEM of the aluminosilicate gel samples sintered at (a) 1400 °C (b) 1500 °C (c) 1600 °C

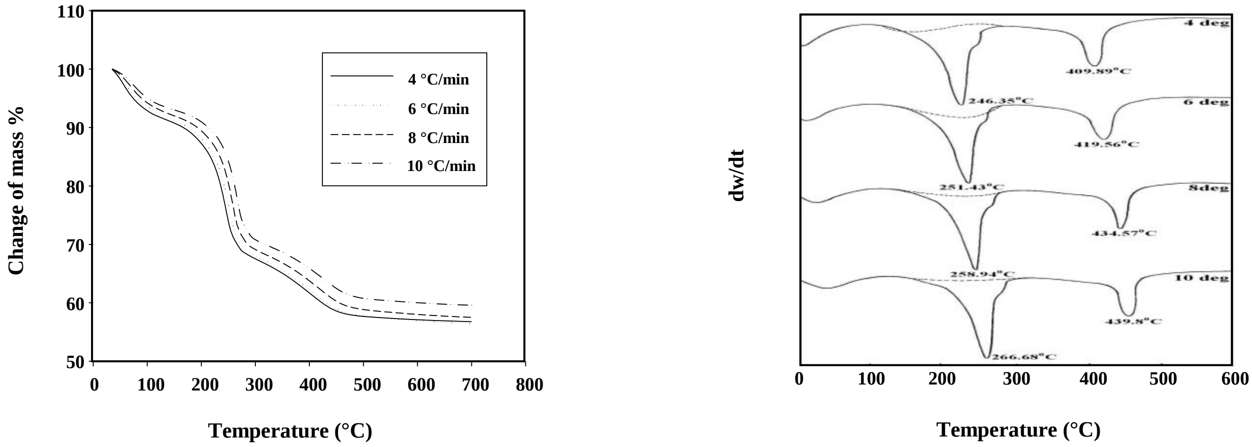

Fig. 5: Scans of (i) TG and (ii) DTG of the aluminosilicate gel at different heating rates.

The TG and DTG scans of the dried gel at heating rates 4, 6, 8 and 10 °C/min have been shown in Fig. 5.

In the plots, two major changes were observed in the temperature range of 35-270°C and 280-490°C. After 500ºC no significant change was observed in the TG plots. So the total dehydration process was divided into two stages and separate calculations were performed for both the stages. From the TG data, fractional decomposition of the sample was calculated. In the first stage, the dehydration was completed with a mass loss of 24% whereas in the second stage almost 8% mass loss was observed.

The initial temperature (t_i), peak temperature (t_m) and final temperature (t_f) of the dehydration process of both the stages were studied for all heating rates. It was observed that in both stages, dehydration temperatures were shifted to higher values with increasing heating rates. This is because at lower heating rates, heat transfer is not so effective and efficient. At higher heating rates, improved and effective heat transfer took place to the inner portions and among the particles. The peak temperature also shifted to higher temperatures with increasing heating rate as a consequence of the increasing rate of volatilization process.

Both Friedman's differential and KAS integral methods predicted that dehydration of the gel in both stages followed second order kinetics (F_2). So the rate of the dehydration is controlled not only by the magnitude of hydroxyl group present in the sample but also by the nature of the gel. The plots of F_2 for both stages obtained by applying Friedman and KAS methods are shown in Figs. 6 and 7 respectively.

Now the other two parameters (activation energy and pre-exponential factor) of the kinetic triplet were calculated by applying the Friedman method and the results are given in Table 1.

The average activation energy for dehydration was found to be lower in stage-1 compared to that of Stage-2.

Table 1: Values of activation energy and Frequency factor based on Friedman Method.

Stage	Heating Rate, ºC/min	Activation Energy, kJ/mole	Exponential Factor A x 10^4
I	4	51.50	8.64
	6	51.43	7.90
	8	50.59	7.62
	10	49.27	4.20
Average		50.70	7.09
II	4	70.61	1.95
	6	70.13	2.26
	8	68.46	2.36
	10	66.92	2.86
Average		69.03	2.36

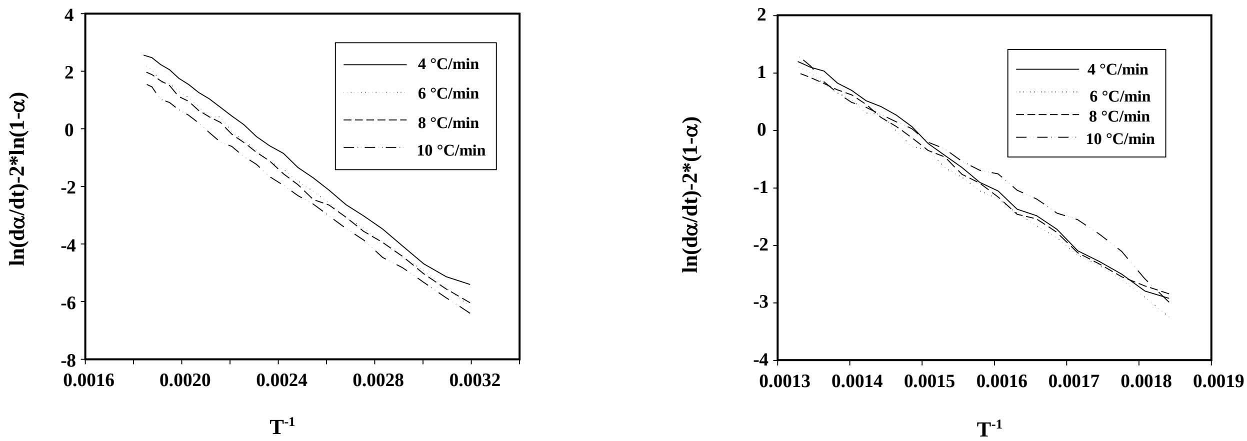

Fig. 6: Friedman Plot based on second order kinetics for (a) Stage-1 and (b) Stage-2 (line fitting).

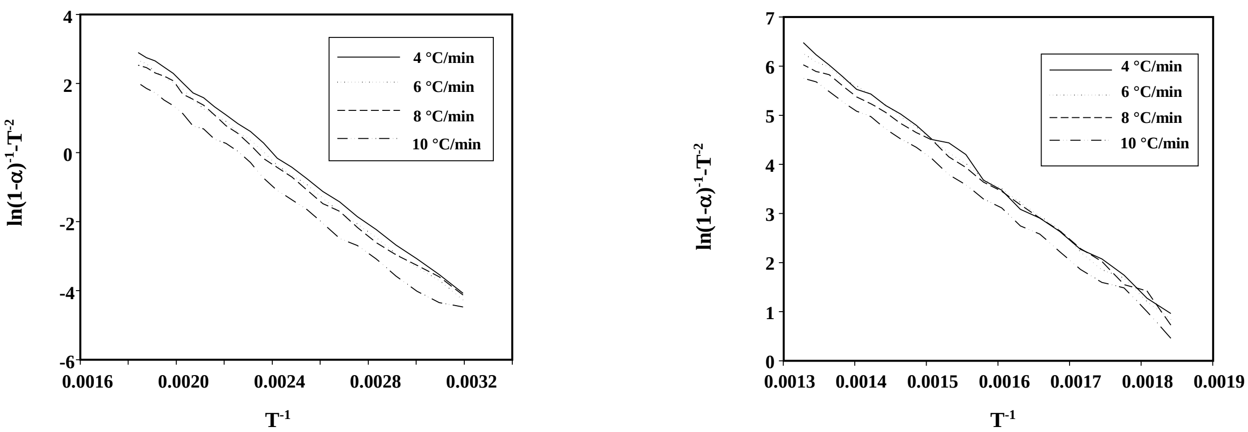

Fig. 7: KAS Plot based on second order kinetics for (a) Stage-1 and (b) Stage-2 (line fitting).

Table 2: Values of activation energy and Frequency factor based on KAS Method.

Stage	Degree of Conversion	Activation Energy (kJ/mole)	Exponential Factor (A x 10^4)
I	0.1	33.68	0.00440
	0.2	24.12	0.00010
	0.3	26.60	0.00009
	0.4	45.44	0.01167
	0.5	60.39	0.49427
	0.6	70.32	6.7798
	0.7	76.34	39.442
	0.8	71.53	16.636
	0.9	70.90	25.908
Average		53.26	9.92
II	0.1	61.23	0.00836
	0.2	81.03	1.1381
	0.3	71.73	0.15202
	0.4	71.21	0.14429
	0.5	80.50	0.8926
	0.6	90.95	8.0802
	0.7	74.63	0.3642
	0.8	82.17	1.4942
	0.9	91.61	12.537
Average		78.34	2.7568

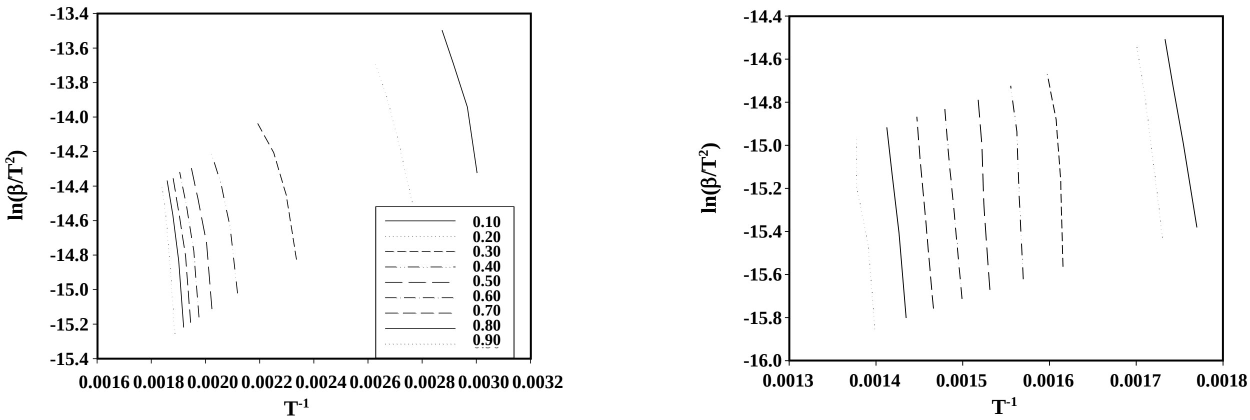

Fig. 8: Isoconversional plots at various conversion degree of gel according to KAS calculation procedure for (i) Phase-1 (ii) Phase-2 to determine activation energy and frequency factor (line fitting).

But the values of the pre-exponential factor which signifies the fraction of activated species participating the reaction was found to much higher in the first stage of dehydration compared to that of the second stage. To determine the activation energy and frequency factor of both stages of the dehydration employing KAS method, the isoconversional plots at various conversion degree of gel were used (Fig.8) and the results obtained are given in Table 2.

The values of activation energy and pre-exponential factor calculated by this method were found to be in good agreement to those calculated by Friedman method. The first stage of dehydration having lower activation energy was assigned to dehydration of Si-OH gel whereas the second stage was considered for the dehydration of Al-OH gel. This is due to the fact that the bond dissociation energy of Al-O (501.9 ± 10.6 kJ/mol) is higher than that of Si-O (452 kJ/mol) [22].

CONCLUSIONS

The dehydration process of aluminosilicate diphasic gel was studied by using thermogravimetric information obtained at multiple heating rates. The dehydration process was accomplished by two distinct stages. Friedman and Kissinger-Akahira-Sunose (KAS) isoconversional methods were applied to determine the values of the kinetic triplet. Both stages of dehydration followed second order kinetics. The first stage of dehydration with lower activation energy and higher frequency factor values were assigned to the dehydration of aluminosilicate gel where as the second stage is associated with the silica gel dehydration process.

Received : Nov. 19, 2017 ; Accepted : Jun. 18, 2018

REFERENCES

[1] Catauro M., Dell'Era A., Ciprioti S. V., Synthesis, Structural, Spectroscopic and Thermoanalytical Study of Sol-Gel Derived SiO_2-CaO-P_2O_5 Gel and Ceramic Materials, *Thermochim. Acta.*, **625**: 20-27 (2016).

[2] H-Escolano M., Ramis X., J-Morales A., J-Diaz M., Suay J., Study of the Thermal Degradation of Bioactive Sol-Gel Coatings for the Optimization of its Curing Process, *J. Therm. Anal. Calorim.*, **107**: 499-508 (2012).

[3] Biedunkiewicz A., Gabriel U., Figiel P., Grzesiak D., Application of Thermal Analysis in Nanotechnology, *J. Therm. Anal. Calorim.*, **101**: 701-706 (2010).

[4] Maitra S., Das S., Ray R., Mitra N. K., Role of Some Transition Metal Cations on the Kinetics of Thermadehydration of Synthetic Zeolites, *Ceram. Int.*, **34**: 485-490 (2008).

[5] Budrugeac P., Muşat V., Segal E., Non-Isothermal Kinetic Study on the Decomposition of Zn Acetate-Based Sol-Gel Precursor, *J. Therm. Anal. Calorim.*, **88**: 699-702 (2007).

[6] Want B., Ahmad F., Kotru P.N., Dielectric and Thermal Characteristics of Gel Grown Single Crystals of Ytterbium Tartrate Trihydrate, *J. Mater. Sci.*, **42**: 9324-9330 (2007).

[7] Jankovic B., Adnadevic B., Jovanovic J., Non-Isothermal Kinetics of Dehydration of Equilibrium Swollen poly(acrylic acid) hydrogel</o:p>, *J. Therm. Anal. Calorim.*, **82**: 7-13 (2005).

[8] Liu H., Ma Q., Liu W., Mechanical and Oxidation Resistance Properties of 3D Carbon Fiber-Reinforced Mullite Matrix Composites Prepared by Sol-Gel Process, *Ceram. Int.*, **40**: 7203-7212 (2014).

[9] Vendange V., Colomban P., How to Tailor the Porous Structure of Alumina and Aluminosilicate Gels and Glasses, *J. Mater. Res.*, **11**: 518-528 (1996).

[10] Sinko K., Poppl L., Transformation of Aluminosilicate Wet Gel to Solid State, *J. Solid. State. Chem.*, **165**: 111-118 (2002).

[11] Leivo J., Meretoja V., Vippola M., Levänen E., Vallittu P., Mäntylä T.A., Sol–Gel Derived Aluminosilicate Coatings on Alumina as Substrate for Osteoblasts, *Acta. Biomater.*, **2**: 659-668 (2006).

[12] Leivo J., Lindén M., Rosenholm J.M., Ritola M., Teixeira C.V., Levänen E., Mäntylä, T.A., Evolution of Aluminosilicate Structure and Mullite Crystallization from Homogeneous Nanoparticulate Sol–Gel Precursor with Organic Additives, *J. Eur. Ceram. Soc.*, **28**: 1749-1762 (2008).

[13] Li S., Zhao X., An Y., Deng W., Hou G., Hao E., Zhou H., Chen J., Effect of Deposition Temperature on the Mechanical, Corrosive and Tribological Properties of Mullite Coating, *Ceram. Int.*, **44**: 6719-6729 (2018).

[14] Islam S., Bidin N., Riaz S., Naseem S., Sanagi M. M., Low Temperature Sol-Gel Based Erbium Doped Mullite Nanoparticles: Structural and Optical Properties, *J. Taiwan Inst. Chem. Eng.*, **70**: 366-373 (2017).

[15] Kaya C., Butler E.G., Selcuk A., Boccaccini A.R., Lewis M.H., Mullite (Nextel™ 720) Fibre-Reinforced Mullite Matrix Composites Exhibiting Favourable Thermomechanical Properties, *J. Eur. Ceram. Soc.*, **22**: 2333-2342 (2002).

[16] Mileiko S.T., Serebryakov A.V., Kiiko V.M., Kolchin A.A., Kurlov V.N., Novokhatskaya N.I., Single Crystalline Mullite Fibres Obtained by the Internal Crystallisation Method: Microstructure and Creep Resistance, *J. Eur. Ceram. Soc.*, **29**: 337-345 (2009).

[17] "Chemical Analysis of Aluminosilicate Refractory Products (Alternative to the X-Ray Fluorescence Method), Part 2: Wet Chemical Analysis": ISO 21587-2: (2007).

[18] Vyazovkin S., Burnham A.K., Criado J.M., Pérez-Maqueda L.A., Popescu C., Sbirrazzuoli N., ICTAC Kinetics Committee Recommendations for Performing Kinetic Computations on Thermal Analysis Data, *Thermochim. Acta.*, **520**: 1-19 (2011).

[19] Velyana G., Zvezdova D., Vlaev L., Non-Isothermal Kinetics of Thermal Degradation of Chitin, *J. Therm. Anal. Calorim.*, **111**: 763-771 (2013).

[20] Roy J., Bandyapadhyay N., Das S., Maitra S., Studies on the Formation of Mullite from Diphasic Al_2O_3-SiO_2 Gel by Fourier Transform Infrared Spectroscopy, *Iran. J. Chem. Chem. Eng. (IJCCE)*, **30**: 65-71 (2011).

[21] Roy J., Maitra S., Synthesis and Characterization of Sol-Gel Derived Chemical Mullite, J. *Ceram. Sci. Tech.*, **5**: 57-62 (2014).

[22] Luo Y.R., "Comprehensive Handbook of Chemical Bond Energies", CRC Press, Boca Raton, FL (2007).